LAWRENCE
LIVERMORE
NATIONAL
LABORATORY

UCRL-JRNL-203530

Development and Characterization of a High Performance Thin-Film Planar Solid-Oxide Fuel Cell Stack

Brandon W. Chung, Christopher N. Chervin, Jeffery J. Haslam, Ai-Quoc Pham, and Robert S. Glass

April 15, 2004

Submitted to Journal of The Electrochemical Society

DISCLAIMER

Development and Characterization of a High Performance Thin-Film Planar Solid-Oxide Fuel Cell Stack

Brandon W. Chung *,†, Christopher N. Chervin‡, Jeffery J. Haslam, Ai Quoc Pham*,#, and Robert S. Glass*

Lawrence Livermore National Laboratory, Chemistry and Materials Science Directorate, Livermore, California 94551, USA

‡ University of California at Davis, Department of Chemistry, One Shields Ave, Davis, California 95616, USA

Abstract

A planar solid oxide fuel cell (SOFC) was fabricated using a tape-cast Ni/yttria-stabilized zirconia (YSZ) anode support, a YSZ thin film electrolyte, and a composite cathode of YSZ and $(La_{0.85}Sr_{0.14})_{0.98}MnO_3$ (LSM). Using pure hydrogen as the fuel gas, a three cell stack with a cross-flow design and external manifolds produced peak power densities of 0.85 W/cm^2 and 0.41 W/cm^2 at 800°C and 700°C, respectively. Using wet methane as the fuel gas, the stack produced a peak power density of 0.22 W/cm^2 at 700°C. Individual cells in the stack showed identical current-voltage (I -V) characteristics. Stack lifetime was limited because of degradation of the cells from oxidation products coming from the metallic interconnect used.

*Electrochemical Society active member

†Contacting author, chung7@llnl.gov, 925-423-3896 (phone), 925-422-6892 (fax)

#Current Address, 3E Systems, 780 Montague Expressway, #305, San Jose, CA 95131

Introduction

Because of their high efficiency and related lower emissions, fuel cells are receiving significant current research interest. Among fuel cell approaches, high temperature solid oxide fuel cells (SOFCs) possess the highest efficiency and the potential for direct conversion of hydrocarbon fuels into electrical energy and heat. A variety of designs for SOFCs have been considered, including tubular, monolithic, and planar. Details of these designs are provided elsewhere.[1] In all cases a fuel cell consists of an anode, electrolyte, and cathode. Interconnects are utilized to electrically connect individual cells in stacks. Typical materials for the SOFC are yttria-stabilized zirconia as the solid electrolyte; Ni-YSZ cermet for the anode; Sr-doped $LaMnO_3$-YSZ as the composite cathode; and lanthanum chromite for the interconnect.

SOFCs do not have the material corrosion and electrolyte management problems associated with fuel cell systems operating at lower operating temperatures[1]. However, some of the materials (in particular, the interconnect) are costly, and this inhibits the commercialization of SOFCs. If the operating temperature could be reduced to 800°C or lower, less expensive materials could be used to fabricate SOFCs. However, as the temperature is lowered, resistive losses across the electrolyte increase, and therefore the cell performance is reduced. To partially overcome this problem, thin film electrolytes are used. However, improvements in power density at lower operating temperatures must still be realized.

A SOFC design that incorporates a flat plate form of electrode support, onto which a thin-film electrolyte is deposited or grown, is referred to as a planar (flat plate) SOFC design. This design promises to capture the important advantages of the SOFC

while easing such problems as materials limitations, fabrication difficulties, and the high manufacturing costs of tubular-design SOFCs. Extensive published results show superior single-cell performances and characterize the physical properties of the fuel cell components.[2–10] In the majority of these published works, however, the cathode or anode support was typically made from die-pressing and sintering ceramic powders into pellets. This process limits the cell footprint to less than a few square centimeters, which cannot be made into practical multi-cell stacks. In addition, previous published works describe scaling up single cells to a multi-cell stack that involved using the YSZ electrolyte as the support layer; however, this has yielded low stack power density because of resistive losses in the relatively thick electrolyte.[11] Alternatively, using a tape-casted anode or cathode for a support, and depositing a thin-film electrolyte, appears to be a promising method to scale up the size of cell for stack applications with minimal resistive loss from the electrolyte.[1]

In prior work, a colloidal spray deposition (CSD) process was demonstrated for depositing thin film electrolytes as well as electrode layers and fabricating larger surface area cells and stacks. [12–14] In addition, we showed that power densities greater than 1 W/cm^2 at 800°C can be achieved in a symmetrical single cell with a pellitized anode support.[12–14] The objective of current work was to demonstrate a high power density planar-type fuel cell stack using the tape-cast anode-support layers and CSD for deposition of the thin film electrolyte and cathode., Individual cells and a stack were tested over a range of temperatures to evaluate performance. In addition to the measured fuel cell power densities, the polarization loss from each cell and interconnect in the stack was determined.

Experimental

Preparation and Characterization of a Single Cell — The anode support was fabricated using YSZ (8 wt% yttria) powder (Tosoh Corp.) mixed with nickel oxide (J. T. Baker) in a ratio of 50/50% by weight. Rice starch (10 wt% of the solids content) was used as a pore former. These components were mixed with proprietary organic binders (dispersant, solvents, binder, and plasticizer) and tape-casted (Richard E. Mistler, Inc., Morrisville, PA) After casting, the green tapes were allowed to air-dry overnight at room temperature, which resulted in an anode approximately 20 mil thick. The tape was then cut to size and partially sintered at 1000°C for 1 hour. These partially sintered tapes served as the anode substrates.

Details of single cell assembly are described elsewhere.[13] Briefly, the partially sintered anode was coated with YSZ electrolyte using the CSD process and the bilayer was then co-fired at 1400°C for 1 hour to produce a fully dense YSZ film on the anode. The cathode was at 50:50 wt.% mixture of $(La_{0.85}Sr_{0.14})_{0.98}MnO_3$ (LSM) powder (Praxair) and YSZ. It was also applied by the CSD process onto the YSZ surface and fired to 1200°C for 1 hour to form a partially sintered layer.

Single cells were tested for electrochemical performance using the test fixture described elsewhere.[13] For single-cell testing, platinum (Pt) mesh was used as current collector and was attached to the electrode surface using Pt paste (Heraeus). Two additional cell voltage probes were attached to both electrodes to avoid measuring the resistance of the Pt lead wires. During testing reduction of NiO to Ni was accomplished *in-situ* in the hydrogen environment, and current-voltage (I-V) measurements were performed at various test temperatures. In addition, a single cell was studied for stability

for 48 hours at 800°C. For this test, an individual cell was first measured for its I-V characteristic and alternately connected to load at 1 A/cm^2 for an hour and then disconnected (allowed to attain OCV for an hour). The cell was held at OCV under 4%H_2-N_2 mixture as the fuel gas overnight. After the programmed cycle, the initial and final (cycled) single cell performances were compared.

Fabrication and Characterization of a Three-cell Stack — Figure 1 shows the structural scheme of the cross-flow planar SOFC stack constructed in our laboratory. Each cell has a 2 × 2-inch footprint with an active area of 18.49 cm^2. Interconnects and endplates are machined from Ducrolloy ($Cr_5Fe_1Y_2O_3$, Plansee Ltd.). Gas manifolds are made from Plansee PM-2000 foil. In the cross-flow design, the fuel cell consists of alternating layers of cells, separated by channeled interconnects, with an endplate having a gas channel on one side. The anode and cathode side of the interconnects are oriented at right angles to each other.[1] Because of the cell's curvature, a small compressive force was applied to the stack to obtain better contact between interconnects and cells. Platinum voltage probes were sandwiched between the interconnect and the cell's cathode to measure polarization from the individual cell, as shown in Figure 2. The assembled layers are sealed with Aremco 571 ceramic sealant and dried overnight under air at room temperature.

Gas manifolds are attached to the sides to duct gases into and out of the stack. Figure 1 shows the inlet and outlet manifolds for fuel gas. For air, only the inlet manifold is needed, because the air output can be exhausted safely without additional gas manifolding. The gas manifolds are also attached to the stack using the Aremco 571 and 516 sealants and are dried overnight under air at room temperature. Electrical

connections are made on the air exhaust side to measure the performance of individual cells in the stack, as shown in Figure 2. To measure stack temperature, thermocouples (Type K) were placed at the top and bottom of the stack. A third thermocouple was placed at the middle of the air exhaust. During measurement resistive heating of the cell causes the temperature to rise. To offset this, the furnace temperature was continuously adjusted to maintain test temperatures using the readings from thermocouples.

The ceramic seal was cured as the stack was brought up to the test temperature (800°C) inside a vertical furnace. While the stack is being brought up to temperature it was purged with nitrogen on the fuel-side and air on the air-side. When the test temperature was reached, the nitrogen flow was changed to 4%H_2–N_2 (balance) mixture. Reduction of NiO to Ni was accomplished *in-situ*. Following reduction to Ni and upon attainment of a stable open circuit voltage (OCV) signal, the fuel gas was switched to 100% H_2.

Results and Discussion

Single Cell Testing—The current-voltage characteristics of a typical symmetric (anode surface area and cathode surface area are equivalent) single cell is shown in Figure 3. The OCV obtained for the single cell at 800°C is approximately 1.2V. This value is dictated by the differences in oxygen partial pressures between the cathode and the anode sides of the cell as described by the Nernst relation.[1] The large value of the OCV for cells fabricated using the CSD technique and the ceramic sealing procedure indicates an absence of pinholes in the electrolyte and a very good seal. The power density measured at 800°C was 0.85 W/cm^2. The cell produced power densities of 0.49 and 0.23 W/cm^2 at 700^{o}C and 650°C, respectively.

The I-V curves shown in Figure 3 indicate both the activation and ohmic polarization features characteristic of all types of fuel cells. The activation polarization is observed at low current densities (<0.2 A/cm^2). At higher current density (>0.2 A/cm^2), the ohmic polarization attributed to the resistance of the electrode and the electrolyte to the transfer of electrons and ions is observed as a linear function of current density. The area-specific resistance measured from the slope of the curve in the ohmic polarization regime is 0.30, 0.44, and 0.86 Ohm-cm^2 at 800, 700, and 650^{o}C, respectively. In contrast to the behavior observed for die-pressed anode pellets,[13] a sharp voltage drop at the highest current density due to concentration polarization is not as noticeable from the tape-cast anode. This is probably related to the thinner anode made by tape casting, which promotes enhanced gas transport compared to the die-pressed anodes.

Stack Performance — To obtain practical power levels for a SOFC, unit cells are connected in electrical series to obtain sufficient voltage. Figure 4 shows the I-V characteristic of a three cell planar SOFC stack. The stack's OCV was stable at 3.34 and 3.38 V at 800 and 700°C, respectively). As expected, when operated under a load, the stack voltage decreased corresponding to the load resistance. As soon as the load was removed, the stack voltage returned rapidly to the initial OCV, indicating that the stack experienced little or no leakage as a result of load cycling. At the test temperatures of 800°C and 700°C, the peak power densities of the stack were 0.85 W/cm^2 and 0.41 W/cm^2, respectively. This is comparable to single cell performance where power densities ranging between 0.80 W/cm^2 and 1W/cm^2 were obtained at 800°C.[12 14] For the three-cell stack, the corresponding output powers were 47 W and 23 W at 800 and 700^{o}C, respectively. The peak power of 47 W at 800°C was obtained at a fuel utilization

efficiency of 60%. The highest power output obtained in prior work in a similar stack was 60 W (1 W/cm^2) at 800°C using dry hydrogen.[14] With further improvements in the fabrication process and modifications in test conditions, a stack performance should approach a single cell performance. In contrast to previous studies,[3, 15] the significance of these results indicates that high performance (power density) obtained for single cells can be translated to a multi-cell stack. Of course, this conclusion is highly dependent on techniques used for cell manufacture and stack design features.

Closer examination of the stack I-V curve shows the ohmic polarization regime around 0.7 A/cm^2 is nonlinear, and this is more noticeable at 800°C. To understand the deviation from the expected linear behavior, each cell and interconnect performance needs to be characterized. Polarization curves for individual cells were recorded during stack testing using the electrical schematic shown in Figure 2. Figure 5(a) shows the polarization losses measured under electrical loads at 800°C. Each cell has similar I-V characteristics during the stack test, which indicates uniformity of test conditions and performance between cells. Each cell polarization includes contributions from both the cell and the interconnect. The interconnect is exposed to hydrogen on the anode side and to air on the cathode side. Figure 5(b) shows the polarization loss from the top endplate/interconnect assembly caused by air oxidation on both sides during the polarization measurement (see Figure 2 for electrical schematic). The I-V curve shows two linear regions with a discontinuity between 0.7 and 1.0 A/cm^2. The initial slope of 0.029 Ohm-cm^2 (below 0.7 A/cm^2) decreases to 0.023 Ohm-cm^2 above 1 A/cm^2. This change in the resistance of the endplate/interconnect at 0.7 A/cm^2 also appears in the I-V curves for the individual cells (Figure 5a). Since this is not observed in single cell

measurements (Figure 3), we attribute the I-V curve changes to oxidation of the interconnect. Under fuel cell testing, the alloy's surface can change by oxidation and/or corrosion processes at test temperatures and may possibly be further influenced by the electrical current flow through the interconnect. This will affect the cell performance. Increased local temperature by the exothermic reaction occuring in the cells can also accelerate the oxidation and/or corrosion processes.

In this work the cell polarization shows small differences between cells and minimal loss due to the interconnect (top end-plate) being exposed to air. However, long-term measurement of Ducrolloy interconnect alloy in air showed continued changes in polarization caused by oxidation and chromium evaporation that degraded the electrode surface,[16] resulting in degradation in stack performance.[14] Replacing the interconnect metal or coating with an appropriate protective layer should improve the stack's lifetime.

The performance of the stack using moist CH_4 (prior to admission into the cell pure methane was bubbled through water at 21 °C) as fuel at 700°C is shown in Figure 6. It has been reported that Ni-based anodes corrode when exposed to hydrocarbon fuels by a process known as metal dusting wherein carbon deposits from the fuel are catalytically graphitized when in contact with a solid metal such as Ni.[17] This process causes the disintegration of bulk metal into metal powder. This was confirmed in a separate experiment where the anode substrate disintegrated into black metal powder under prolonged exposure to the moist CH_4, indicating that the cell can be tested for only a short duration. In our work, comparing to the OCV in dry, pure hydrogen (3.38 V), the OCV of the stack with the moist CH_4 as fuel gas was somewhat lower at 3.21 V. The

peak power density was more significantly affected, being only 0.22 W/cm^2. Following measurement in moist CH_4, dry hydrogen was reintroduced as the fuel gas. Subsequent measurement showed no degradation of the OCV and insignificant loss of peak power density (the stack re-attained a power density of approximately 0.4 W/cm^2) indicating that the relatively brief measurements using moist methane did not cause significant degradation to the anode during the measurement. It has recently been shown that Cu cermets or ceria-based anode materials appear to show improved tolerance to methane, but the measured single-cell power densities were quite low in these studies.[18, 19]

Cell Stability — We have shown that a high-performance stack can be fabricated;[14] however, the performance decays with time largely because of interconnect degradation. To determine if the observed degradation is also caused in part by degradation at the electrode/electrolyte, or at interfaces, an investigation was conducted to measure individual cell stability under prolonged operation. For this test, an individual single cell was cycled seven times between electrical load (1 A/cm^2) and OCV during 48 hours of testing. As a result of this programmed cycling, the cell performance degraded from initial 0.81 W/cm^2 to 0.61 W/cm^2, as shown in Figure 7. Additional load/OCV cycling did not appear to cause further degradation in the power density. Clearly, further improvement in cell materials and construction is needed to attain long-term performance goals. Since the cell's performance appears to stabilize after two days of operation, the continued decay observed in the stack performance is attributed in large part to degradation in the interconnect.

AC impedance spectroscopy was carried out to resolve which interface or component of the cell contributed most to the cell degradation. Figure 8 shows the

complex impedance plots on the cell (a) before and (b) after the degradation of the cell corresponding to the second day of testing shown in Figure 7. The plots show two electrode arcs formed between the high- and low-frequency impedance intercept, representing the polarization loss associated with both electrodes. The high-frequency intercept of the electrode arcs yields the ohmic resistance, 0.16 Ohm-cm^2 (obtained by multiplying the high-frequency intercept by the cathode area of 1.35 cm^2). Since the measurement was conducted using a four-wire configuration, this represents the electrolyte resistance. Tsai *et al*. reported a similar value for ohmic resistance of a thin-film YSZ electrolyte on a cathode support.[20] From testing with different atmospheres in the cathode (air, O_2) and anode (100% H_2, 4%H_2+N_2, CH_4), the two arcs, R1 and R2, are ascribed to polarization losses in the cathode and anode, respectively. As seen in the plot, upon continued testing significant change in resistance occurred within the anode, with the resistance R2, extracted from impedance analysis by curve fit, increasing from 1.7 Ohm-cm^2 to 6.4 Ohm-cm^2 following 48 hours of testing. From this analysis, the main degradation in the cell performance during the initial load cycling can be ascribed to degradation in the anode or at the anode-electrolyte interface. Further investigation of the degradation mechanisms of both single cell and stack under electrical loads is underway.

In summary, it has generally been observed that the power densities measured in stacks are less than that measured in single cells. A number of factors might be responsible for this: imperfect contact of the cells with the interconnect; interconnect resistance; gas flow distribution; and morphological difference or changes in the cell components during fabrication and testing. Although single-cell tests are useful for basic

studies, only the performance obtainable in a stack has real significance for practical applications.

In this and in a previous study,[14] we have demonstrated that high stack power densities are obtainable at temperatures below 1000^{o}C. In part, we attribute this to favorable material microstructural properties resulting from the use of the CSD process to deposit the thin-film electrolyte and cathode. Additional improvements are anticipated by optimizing the microstructure of the anode and other cell processing conditions.

Additional work is required to understand the mechanism of the fuel cell degradation under prolonged operation. AC impedance measurements made under fuel cell load will be a useful technique to employ. Whether the electrode microstructure changes under constant operation or whether any secondary chemical reactions occur needs to be answered.

Conclusions

We have demonstrated that the high performance of thin-film single SOFCs can be realized in a symmetrical multi-cell stack at temperatures ranging from 650-800^{o}C. Using pure hydrogen as fuel gas, a three-cell stack with a cross-flow design and external manifolds produced peak power densities of 0.85 W/cm^2 and 0.41 W/cm^2 at 800°C and 700°C, respectively. This compares to single-cell values of 0.85 W/cm^2 and 0.49 W/cm^2 at 800^{o}C and 700^{o}C, respectively. Using wet methane as the fuel gas, the stack produced a peak power density of 0.22 W/cm^2 at 700°C. High stack performance is attributed to the use of electrodes and electrolytes having favorable material properties and attention to cell construction details. In this study, each cell in the stack showed the same I-V

characteristics, indicating uniformity of the cell fabrication using the techniques employed in this work. AC impedance studies indicated that resistance increase at the anode/electrolyte interface degrades cell performance during fuel-cell operation. In addition, oxidation of the interconnect at temperatures above 700°C also limits the stack lifetime. Further improvements in the electrodes, interfaces, and interconnect are needed for long-term operation of a multi-cell stack without significant degradation at the temperatures used in this study.

Acknowledgments

This work was performed under the auspices of the U.S. Department of Energy by University of California Lawrence Livermore National Laboratory under contract no. W-7405-Eng-48.

References

1. N. Q. Minh, *J. Am. Ceram. Soc.*, **76**, 563 (1993).
2. N. Minh, K. Barr, P. Kelly, and K. Montgomery, in *Proceedings of 1996 Fuel Cell Seminar*, p. 40, Courtesy Associates, Washington, DC (1996).
3. N. Minh, A. Anumakonda, B. Chung, R. Doshi, J. Ferrall, J. Guan, G. Lear, K. Montgomery, E. Ong, and J. Yamanis, in *Proceedings of the 6th International Symposium on Solid Oxide Fuel Cells*, S. C. Singhal and M. Dokiya, Editors, PV 99-19, p. 68, The Electrochemical Society Proceedings Series, Pennington, NJ, USA (1999).
4. S. de Souza, S. J. Visco, and L. C. De Jonghe, *Solid State Ionics*, **98**, 57 (1997).
5. J. W. Kim, A. V. Virkar, K. Z. Fung, K. Mehta, and S. C. Singhal, *J. Electrochem. Soc.*, **146**, 69 (1999).
6. H. Arai, K. Eguchi, T. Setoguchi, R. Yamaguchi, K. Hashimoto, and H. Yoshimura, in *Proceedings of the 2nd International Symposium on Solid Oxide Fuel Cells*, F. Grosz, P. Zegers, S. C. Singhal, and O. Yamamoto, Editors, p. 167, Athens, Greece, 2–5 July 1991, Commission of the European Communities (1991).
7. H. Sasaki, M. Suzuki, S. Otoshi, A. Kajimura, and M. Ippommatsu, *J. Electrochem. Soc.*, **139**, L12 (1992).
8. J. W. Kim and A. V. Virkar, in *Proceedings of the 6th International Symposium on Solid Oxide Fuel Cells*, S. C. Singhal and M. Dokiya, Editors, PV 99-19, p. 830, The Electrochemical Society Proceedings Series, Pennington, NJ, USA (1999).

9. J. P. Ouweltjes, F. P. F. van Berkel, P. Nammensma, and G. M. Christie, in *Proceedings of the 6th International Symposium on Solid Oxide Fuel Cells,* S. C. Singhal and M. Dokiya, Editors, PV 99-19, p. 803, The Electrochemical Society Proceedings Series, Pennington, NJ, USA (1999).

10. D. Ghosh, G. Wang, R. Brule, E. Tang, and P. Huang, in *Proceedings of the 6th International Symposium on Solid Oxide Fuel Cells,* S. C. Singhal and M. Dokiya, Editors, PV 99-19, p. 851, The Electrochemical Society Proceedings Series, Pennington, NJ, USA (1999).

11. T. L. Wen, D. Wang, M. Chen, H. Tu, Z. Lu, Z. Zhang, H. Nie, and W. Huang, *Solid State Ionics*, **148**, 513 (2002).

12. J. J. Haslam, A. Q. Pham, B. W. Chung, and R. S. Glass, *J. Am. Ceram. Soc*., accepted for publication.

13. B. W. Chung, A. Q. Pham, J. J. Haslam, and R. S. Glass, *J. Electrochem. Soc.*, **149**, A325 (2002).

14. A. Q. Pham, B.W. Chung, J. J. Haslam, D. J. Lenz, E. F. See, and R. S. Glass, in *Proceedings of the 7th International Symposium on Solid Oxide Fuel Cells,* S. C. Singhal and H. Yokokawa, Editors, PV 2001-16, p. 148, The Electrochemical Society Proceedings Series, Pennington, NJ, USA (2001).

15. A. V. Virkar, N. S. Kaput, J-F. Jue, G-Y. Lin, D. M. England, P. Smith, D. W. Prouse, and K. K. Shetty, in *Proceedings of the 1999 Review Conference on Fuel Cell Technology*, Electric Power Research Institute/Gas Research Institute/Department of Energy, Aug 3-5, 1999.

16. E. Batawi, W. Glatz, W. Kraussler, and M. Janousek, in *Proceedings of the 6th International Symposium on Solid Oxide Fuel Cells*, S. C. Singhal and H. Yokokawa, Editors, PV 99-16, p. 731, The Electrochemical Society Proceedings Series, Pennington, NJ, USA (1999).

17. C. M. Chun, J. D. Mumford, and T. A. Ramanarayanan, *J. Electrochem. Soc.*, **147**, 3680 (2000).

18. S. Park, R. Craciun, J. M. Vohs, and R. J. Gorte, *J. Electrochem. Soc.*, **146**, 3603 (1999).

19. E. Perry Murray, T. Tsai, and S. A. Barnett, *Nature*, **400**, 649 (1999).

20. T. Tsai and S. A. Barnett, *Solid State Ionics*, **93** , 207 (1997).

Figures

Figure 1

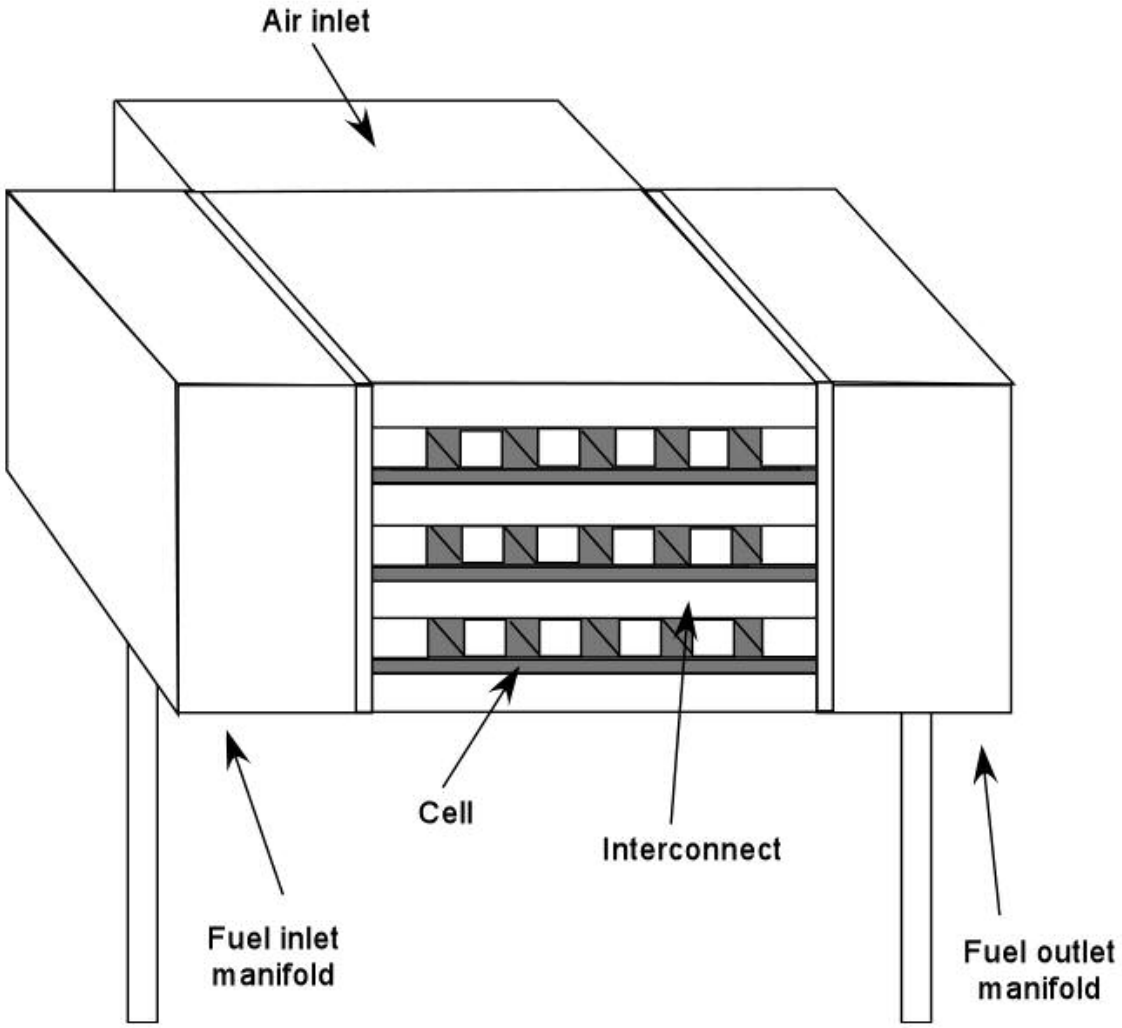
Air inlet
Cell
Interconnect
Fuel inlet manifold
Fuel outlet manifold

Figure 2

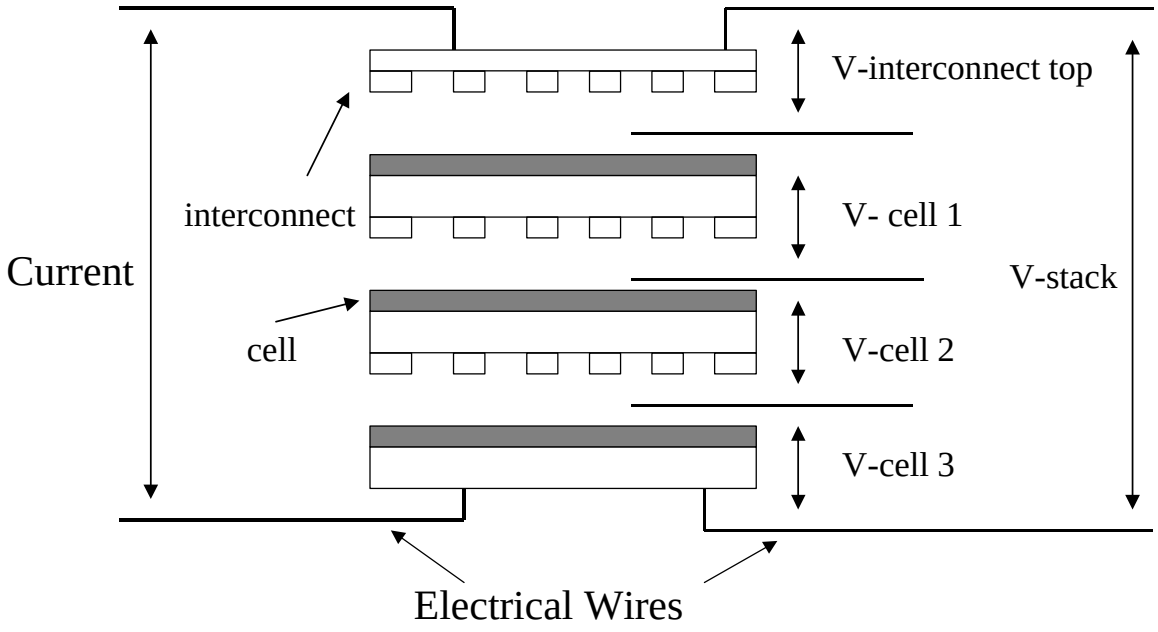
V-interconnect top
interconnect
Current
V- cell 1
V-stack
cell
V-cell 2
V-cell 3
Electrical Wires

Figure 3

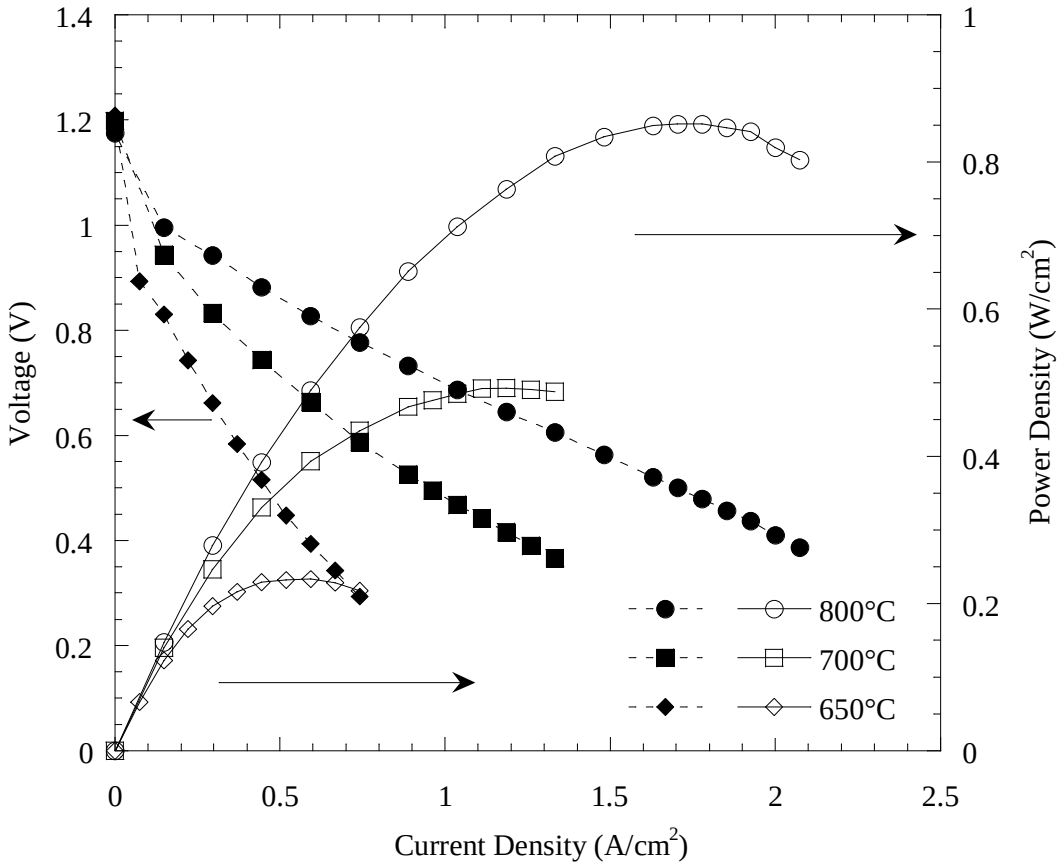
Voltage (V)
Power Density (W/cm^2)
Current Density (A/cm^2)
800°C
700°C
650°C
0
0.2
0.4
0.6
0.8
1
1.2
1.4
0.5
1.5
2
2.5

Figure 4

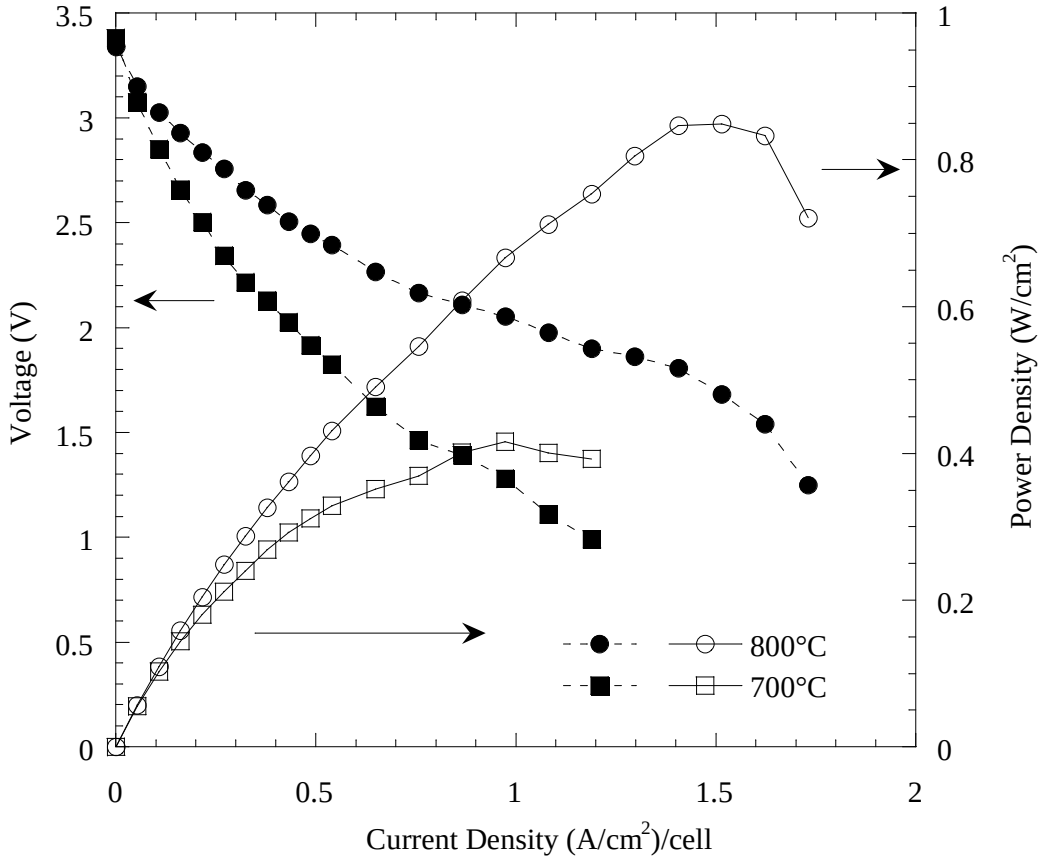
Voltage (V)
Power Density (W/cm^2)
Current Density (A/cm^2)/cell
800°C
700°C
0
0.5
1
1.5
2
2.5
3
3.5
0.2
0.4
0.6
0.8

Figure 5a

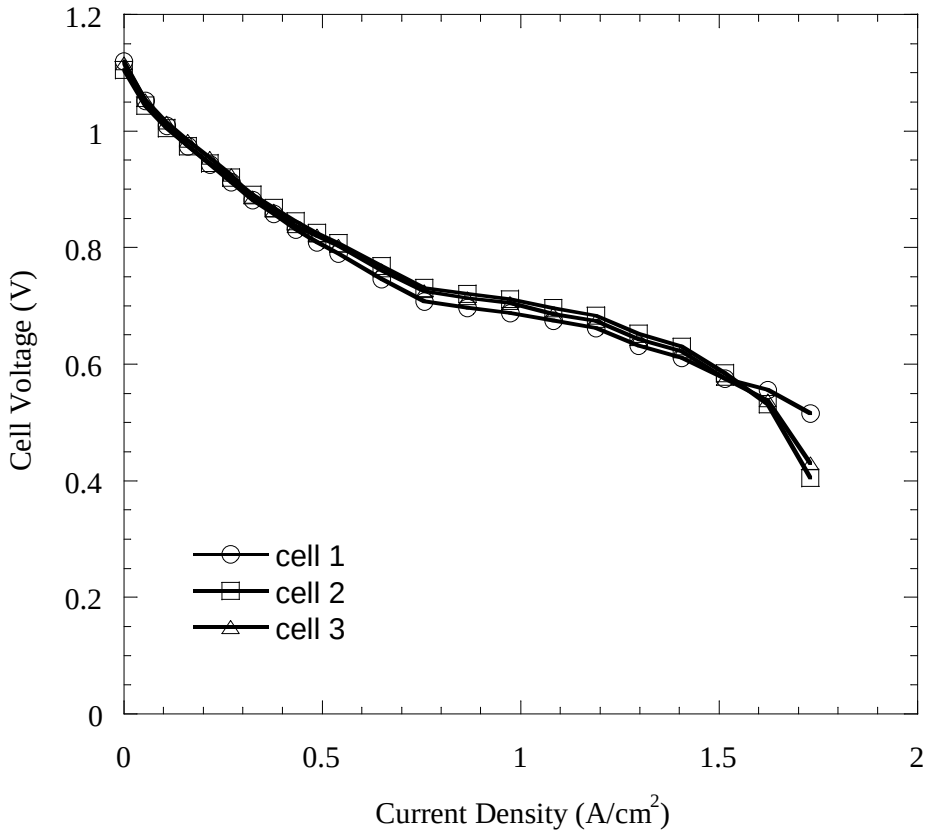
1.2
1
0.8
0.6
0.4
0.2
0
Cell Voltage (V)
0
0.5
1
1.5
2
Current Density (A/cm2)
cell 1
cell 2
cell 3

Figure 5b

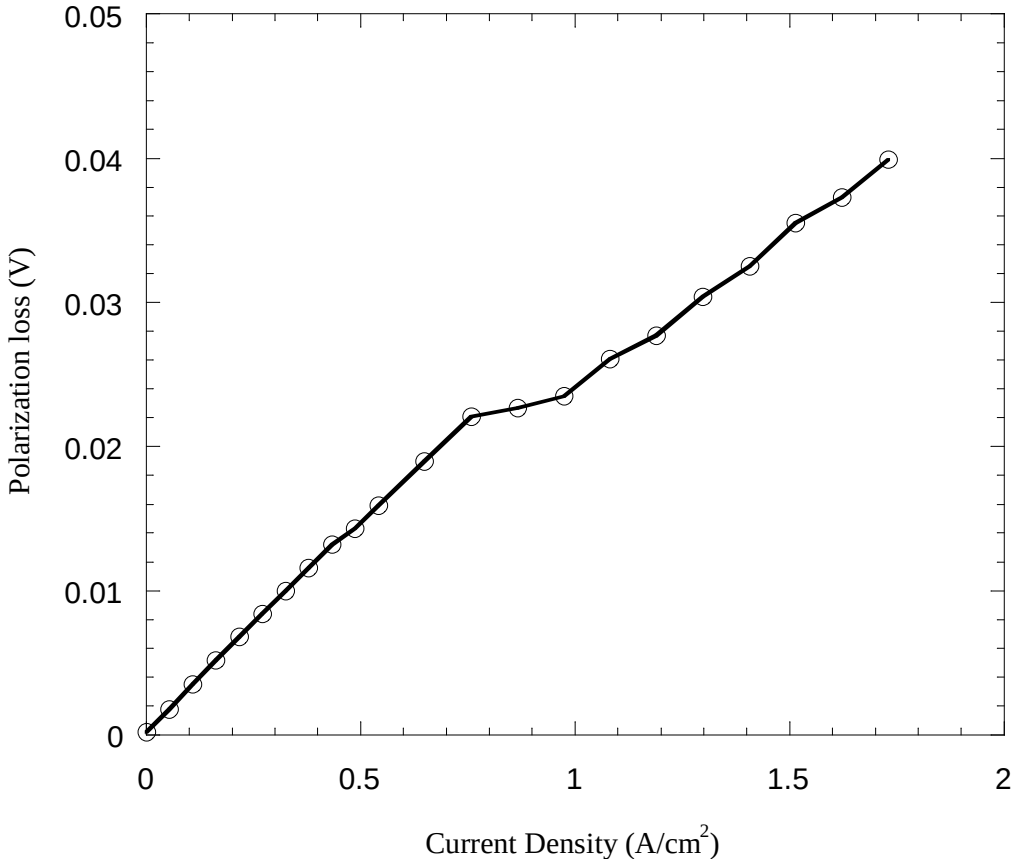
0.05
0.04
0.03
0.02
0.01
0
Polarization loss (V)
0
0.5
1
1.5
2
Current Density (A/cm2)

Figure 6

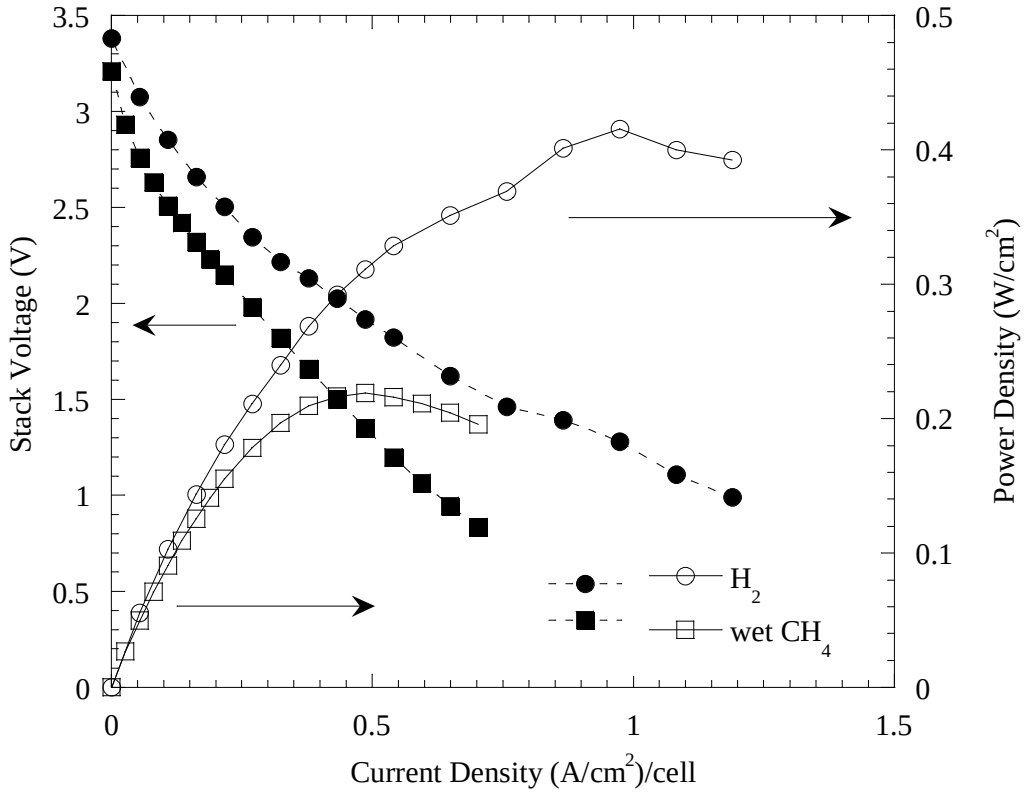
Stack Voltage (V)
Power Density (W/cm^2)
Current Density (A/cm^2)/cell
H$_2$
wet CH$_4$
0
0.5
1
1.5
2
2.5
3
3.5
0.1
0.2
0.3
0.4

Figure 7

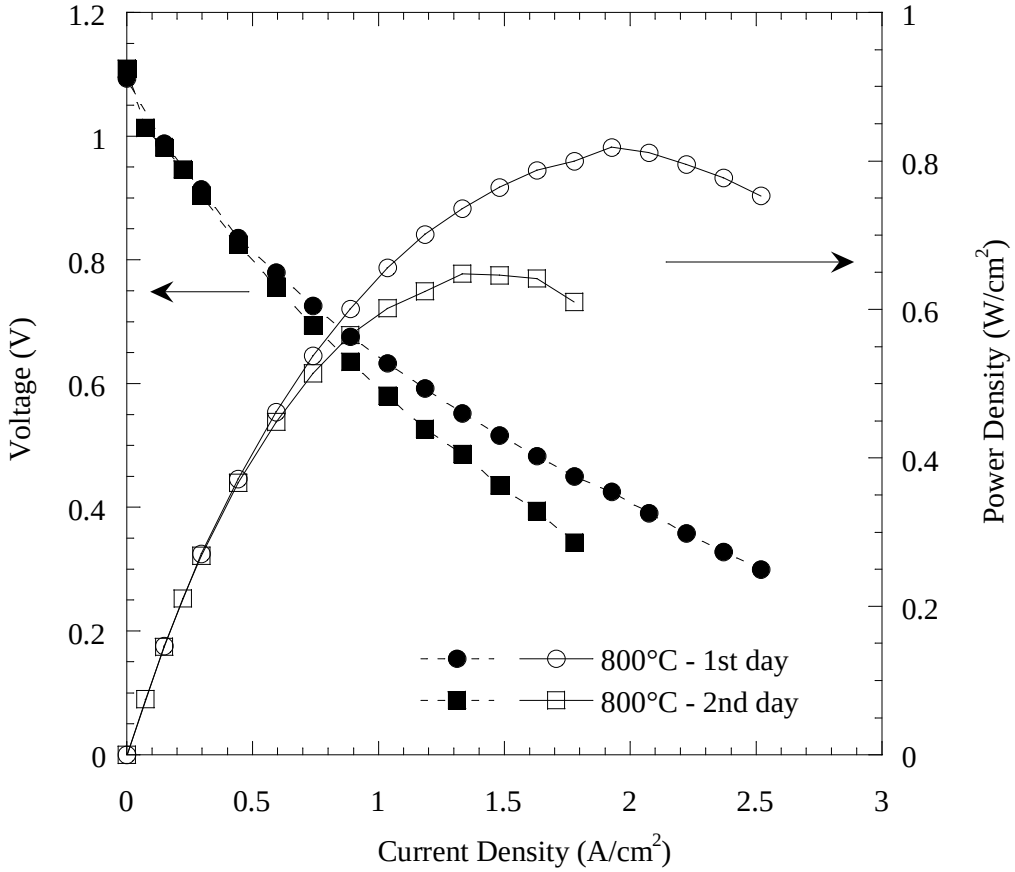
1.2
1
0.8
0.6
0.4
0.2
0
Voltage (V)
1
0.8
0.6
0.4
0.2
0
Power Density (W/cm2)
0
0.5
1
1.5
2
2.5
3
Current Density (A/cm2)
800°C - 1st day
800°C - 2nd day

Figure 8

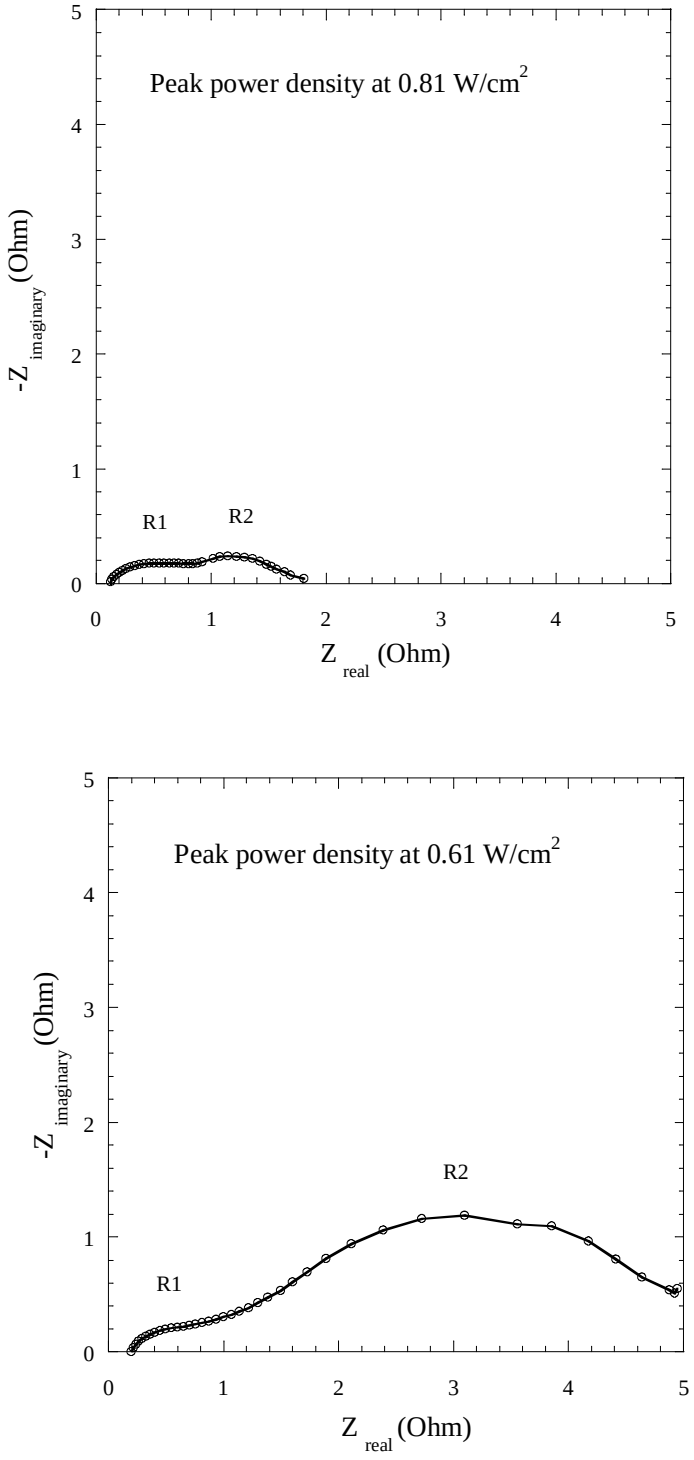
Peak power density at 0.81 W/cm2
-Z imaginary (Ohm)
Z real (Ohm)
R1
R2
Peak power density at 0.61 W/cm2
-Z imaginary (Ohm)
Z real (Ohm)
R1
R2